A Study on the Behavior of Evaporating Diesel Spray Using LIEF Measurement and KIVA Code

Jeongkuk Yeom*, Sungsik Chung, Jongyul Ha
Department of Mechanical Engineering, Dong-A University, Busan 604-714, Korea
Yongrae Kim
School of Mechanical and Aerospace Engineering, Graduate School, Seoul National University, Seoul, 151-742, Korea
Kyoungdoug Min
School of Mechanical and Aerospace Engineering, Seoul National University, Seoul, 151-742, Korea

The effects of change in injection pressure on spray structure in high temperature and pressure field have been investigated. The analysis of liquid and vapor phases of injected fuel is important for emissions control of diesel engines. Therefore, this work examines the evaporating spray structure using a constant volume vessel. The injection pressure is selected as the experimental parameter, is changed from 400 bar to 800 bar by using a common rail injection system. Also, we conducted simulation study by modified KIVA-II code. The results of simulation study are compared with experimental results. The images of liquid and vapor phase for free spray were simultaneously taken by exciplex fluorescence method. As experimental results, the vapor concentration of injected fuel is leaner due to the increase of atomization in the case of the high injection pressure than in that of the low injection pressure. The calculated results obtained by modified KIVA-II code show good agreements with experimental results.

Key Words : Exciplex Fluorescence Method, KIVA-II Code, Diesel Spray, Mie Scattering, Common Rail

Nomenclature

K : Ratio of the Particle's Distortion Energy to Its Total Energy
LIEF : Laser Induced Exciplex Fluorescence
SMD : Sauter Mean Diameter

Greek symbols

Φ : Degree of Freedom
ρ : Density of Ambient Gas

Subscripts

a : Ambient Gas
inj : Injection
liq : Liquid Phase
vap : Vapor Phase
10 : Arithmetic Average

* Corresponding Author,
E-mail : ejk6804@korea.com
TEL : +82-51-200-7654; **FAX** : +82-51-200-7656
Department of Mechanical Engineering, Dong-A University, Busan 604-714, Korea. (Manuscript **Received** July 9, 2004; **Revised** October 8, 2004)

1. Introduction

In diesel engines, atomization, evaporation, and mixture formation process of injected fuel affect ignition characteristics and combustion process. However, the process and structure of injected spray have not been cleared yet due to the unsteady flow processes of injected fuel which are high pressure injection, breakup, atomization, and turbulent entrainment process of ambient gas. The papers about development mechanism of diesel spray have been reported (Wakuri et al., 1959 ; Hiroyasu et al., 1978 ; Hiroyasu and Arai, 1980 ; Dan et al., 1997). However, the previous

studies have limitation such as non-reacting diesel spray (Hiroyasu et al., 1978 ; Hiroyasu and Arai, 1980 ; Dan et al., 1997) and Wakuri et al. (1959) conducted a study for relatively lower injection pressure. Therefore, this study examines the evaporating spray structure using a constant volume vessel with high temperature and pressure field. On the other hand, in the field of spray structure and spray combustion, the simple models were suggested for various simulation schemes, such as KIVA (KIVA-II, KIVA-3, and KIVA-3V) (Amsden et al., 1985 ; 1989 ; Amsden, 1993 ; 1997) proposed by the Los Alamos Lab. and STAR-CD (Ahmadi-Befrui et al., 1996). In this study, the KIVA-II code was used in simulation analysis. The TAB model of KIVA-II code was modified by simultaneously tuning the χ-squared distribution function with variation in the degree of freedom Φ and the ratio of the particle's distortion energy to its total energy K in the non-evaporating diesel spray (Senda et al., 1997). From the TAB model results of a non-evaporating diesel spray obtained by setting $\Phi=6$ and $K=0.89$ agreed well with the experimental results. The Φ and K of the modified TAB model used in this study are 6 and 0.89 respectively, as in the non-evaporating spray. To verify the validity of the KIVA-II code analysis, the results obtained by using the KIVA-II code were also compared with the experimental results.

2. Experimental Apparatus and Analysis Procedure

Figure 1 shows the schematic diagram of an experimental apparatus including a constant volume vessel and optical instruments. The spray experiment was conducted in a high pressure and high temperature condition, which was essential for evaporating spray. This ambient gas condition was made inside a constant volume vessel by using heaters and highly pressurized nitrogen gas. Nitrogen was used as an ambient gas to prevent a quenching effect of liquid fluorescence by oxygen. The vessel was covered with insulators and had quartz glass windows to visualize a spray. A common rail injector which had a 6-hole nozzle

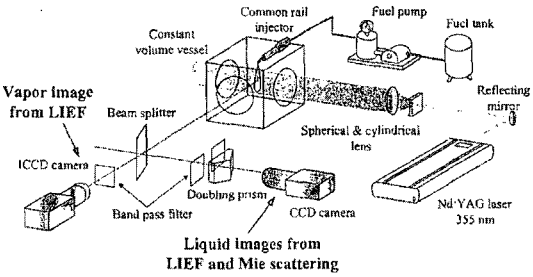

Fig. 1 Schematic of experimental apparatus

was installed at the side of a vessel. The injector nozzle was covered with a metal cap, which had one large hole fitted to a target nozzle hole and five holes connected with steel tubes. As a result, only one spray among six sprays could be visualized without the interference of a laser beam. The nozzle hole diameter was 0.22 mm and the length of the hole was 0.8 mm. In this experiment the TMPD/naphthalene exciplex system was used for LIEF technique. The fuel was composed of 90% *n*-tetradecane ($C_{14}H_{30}$, B.P.= 526 K), 9% naphthalene ($C_{10}H_8$, B.P.=491 K), and 1% TMPD (N,N,N′,N′ tetramethylene-p-phenylene diamine, $C_{10}H_{16}N_2$, B.P.=533 K) by weight. N-tetradecane was selected as a base fuel to coincide with a boiling temperature of the fuel and TMPD. The Nd : YAG laser of the third harmonic (355 nm) was used as a light source and a sheet beam was focused to cover the whole length of the spray by spherical and cylindrical lenses. A beam splitter was installed in front of the vessel so that the radiated light from the spray could be equally separated into two perpendicular directions. Then a vapor image from LIEF was photographed by an ICCD camera, and liquid images from LIEF and Mie scattering were photographed by a CCD camera. In order to photograph two images simultaneously in one screen, a doubling prism was located in front of the CCD camera. The fluorescent emissions from vapor and liquid phase peaked at 400 nm and 480 nm. Hence, band pass filters, which had center wavelengths of 390 nm and 532 nm, were used to capture the vapor image and the liquid image from LIEF respectively, and a band pass filter centered at 354.7 nm was used to capture the liquid image from Mie scattering. Therefore total

Table 1 Experimental conditions

Injection nozzle	Diameter of hole d_n (mm) 0.22			
	Length of hole L_n (mm) 0.80			
Ambient gas		N_2 gas		
Ambient temperature	T_a (K)	650		
Ambient pressure	p_a (bar)	25		
Ambient density	ρ_a (kg/m^3)	13.2		
Injection pressure	p_{inj} (bar)	400	600	800
Injection duration	t_{inj} (ms)	1.60	1.20	1.00
Injection quantity	Q_{inj} (mg)	8 (per hole)		

Table 2 Simulation conditions

Injection pressure	p_{inj} (bar)	400	600	800
Injection velocity	u_{inj} (m/s)	172.3	213.4	247.8
Injection duration	t_{inj} (ms)	1.6	1.2	1.0
Injection quantity	Q_{inj} (mg)	8.0		
Initial droplet temperature	T_{pi} (K)	293		
Fuel		n-Tetradecane ($C_{14}H_{30}$)		
Number of parcel	N_p	1000		
Ambient temperature	T_a (K)	650		
Ambient density	ρ_a (kg/m^3)	13.2		
Number of mesh		32×1×70 (sector mesh)		

three images could be acquired simultaneously in one spray event. The injection pressure was varied to examine their effects for an air-fuel mixing process and the development of the evaporating diesel spray. The ambient gas temperature was 650 K.

2.1 Experiment condition

The injection was varied to investigate the effect of the injection pressure and the ambient gas pressure in the air-fuel mixing process and the development of the evaporating diesel spray. The quantity of injected fuel from one hole was kept at 8 mg with the injection pressure by changing the injection duration. This fuel quantity corresponds to the quantity injected at the full load in the small sized D.I. diesel engine. Detail experimental conditions are listed in Table 1.

2.2 Simulation condition

Table 2 shows calculation condition used in this study. The used fuel is also n-tetradecane (as in experimental case). The injection quantity and density of ambient gas are 8 mg and ρ_a= 13.2 kg/m^3 respectively, as shown in Table 2. These values correspond with those in the experiment as mentioned above.

3. Results and Discussion

3.1 Experimental analysis

Figure 2 shows the results of three images captured simultaneously and a relative SMD (Sauter Mean Diameter) distribution. The spray image represents the typical diesel spray, which contains a meandering flow due to the entrainment by external gases. Comparing two liquid images from LIEF and Mie scattering, there is not much difference between two images. This indicates that the liquid image from LIEF was acquired exactly, for Mie scattering technique is a sure method to measure the liquid phase. Meanwhile, the relative SMD can be obtained by dividing the fluorescence intensity by the scattering intensity in the liquid image. It is because the fluorescence intensity is proportional to the cube of the droplet diameter and the scattering intensity is proportional to the square of that.

Figure 3 shows the two-dimensional fluorescence intensity images of the free spray with injection pressure change obtained by exciplex fluorescence method. In the figures, the left side is the liquid phase and the right side is vapor phase,

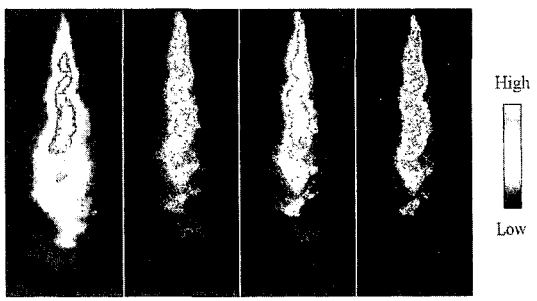

Fig. 2 Spray images and relative SMD distribution

respectively. The top of spray images is invisible by about 5 mm due to the cap covered at the nozzle tip. All the graphs for experimental results were plotted on the average 6 images. The photographing timing was set when the injected fuel mass was almost the same in the each injection pressure. There is not much difference among images taken at different injection pressure in terms of structure and spray tip penetration. However, the fluorescence intensity of the liquid phase rapidly decreases in the vicinity of about 35 mm from the nozzle tip. Also, in each condition of injection pressure, the meandering flow of the mainstream region starts on the spray radial direction at the distance of about 35 mm from the nozzle tip. As a result, it could be speculated that the transition point at which the momentum of the spray interchanges with the ambient gas is, approximately, in the vicinity of 35 mm. Consequently, the vortex flow of the ambient gas dominates spray development in the latter part of the injection.

Figure 4 shows the temporal change in spray tip penetration of the vapor and liquid phase. The

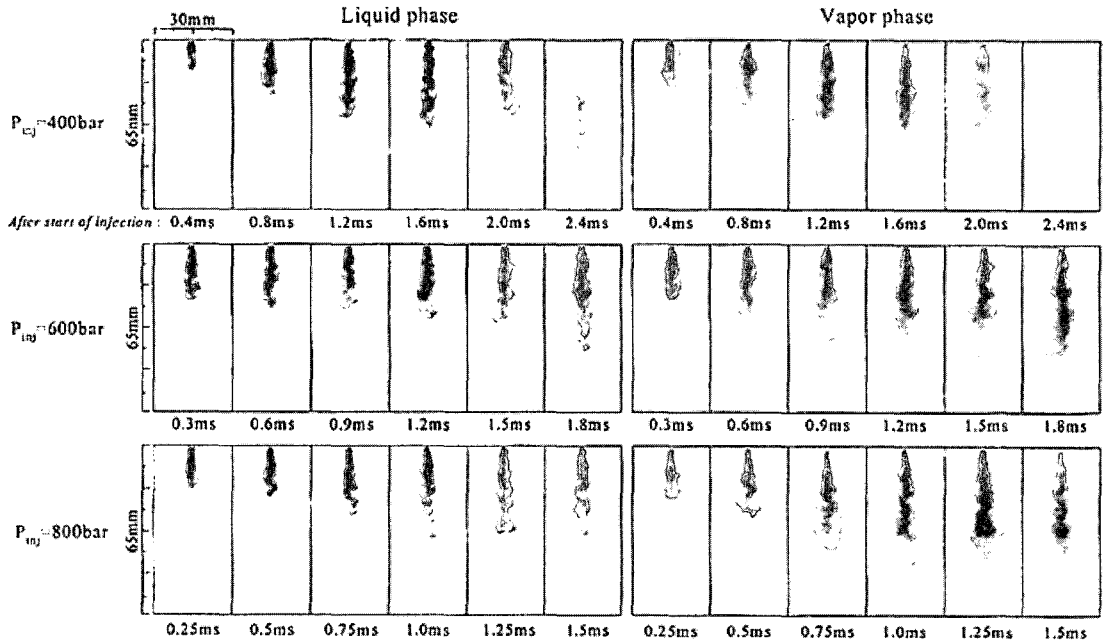

Fig. 3 Spray images with change of injection pressure (p_a=25 bar)

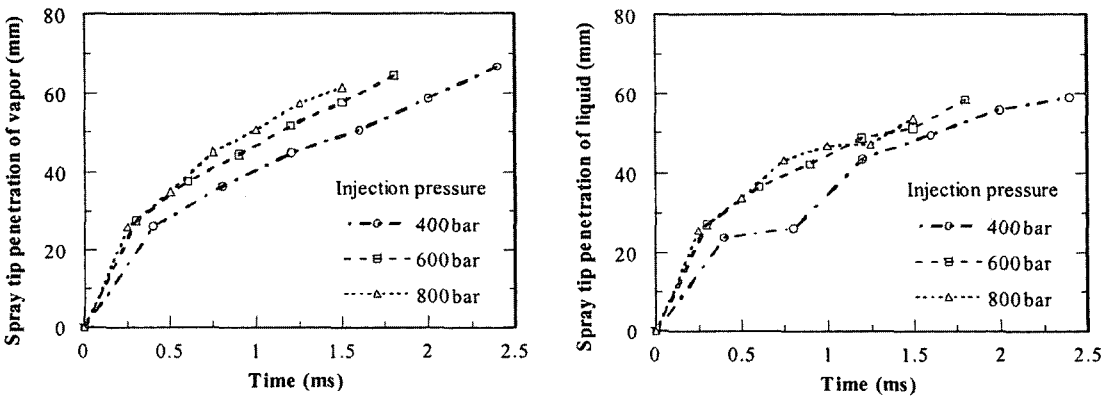

Fig. 4 Spray tip penetration with change of injection pressure

spray tip penetrations of liquid phase and vapor are determined by the overall fluorescence intensity region in the images. In the figure, with the same mass of fuel in the injected spray, the spray tip penetration does not depend on injection pressure, the same as a non-reaction diesel spray (Dan et al., 1996). The penetration of liquid phase increase with elapsing time. A convergence tendency of the liquid phase length value, as shown in the other experiments using evaporating spray (Hodges et al., 1991 ; Baritaud et al., 1994 ; Espey et al., 1994 ; Espey and Dec, 1995 ; Espey et al., 1997), could not be observed. Hence, we conducted a tuning for images of liquid phase, and the result is presented in Fig. 5.

Figure 5 shows the liquid length versus the elapsing time. In the figure, the liquid length is defined by the spatial region where fluorescence intensity marked by maximum intensity of the spray's center decreases to 10% of it value in each image. Also, with regard to the length of the liquid phase spray, there are several empirical formulas induced through the experiment results. The following equation is Hiroyasu's.

$$l_{liq}=2.95\left(\frac{\Delta P}{\rho_a}\right)^{\frac{1}{4}}(d_n t)^{\frac{1}{2}}$$

Where ΔP is injection pressure, ρ_a is density of ambient gas, and d_n is nozzle hole diameter. The results obtained by applying the experimental conditions to this equation and the liquid lengths from the experiment results are compared in Fig. 5. As shown in Fig. 5, the value of the liquid length is almost 35 mm in the curve, because the

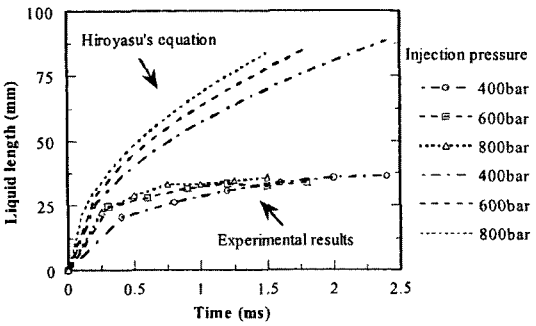

Fig. 5 Liquid length compared with Hiroyasu's equation

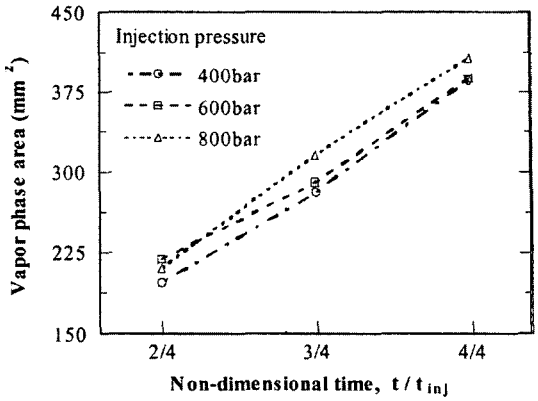

Fig. 6 Temporal change of vapor phase area

atomization of spray is promoted by injection of higher pressure. Hence, vaporization acceleration due to the high pressure injection brings about the convergence tendency of liquid length regardless of the change of injection pressure. Namely, the ambient gas entrainment into inner spray occurs actively in the case of high pressure injection. As a result, the liquid length as measured in Fig. 5 is equal to the liquid lengths of experiments (Hodges et al., 1991 ; Baritaud et al., 1994 ; Espey et al., 1994 ; Espey and Dec, 1995 ; Espey et al., 1997). Also the behavior tendency of liquid length can be found at the start point of spray development in the radial direction as shown in Fig. 3. This means that the distance of 38 mm from nozzle exit corresponds to the end of momentum exchange from the liquid jet to the ambient gas in non-evaporating spray (Dan et al., 1997). There is much difference between two results, because the equation of Hiroyasu was based on the experiment results acquired in non-evaporating condition. The area in which the vapor phase occupied was calculated as shown in Fig. 6. The vapor area increases as the injection pressure increases, because the atomization and evaporation of the diesel spray are promoted by the increase of shear force caused by the interaction between the injected fuel and ambient gas. Hence, it could be speculated that the high pressure injection excellently causes mixture formation. Therefore, the highly pressurized injection gives a profitable condition to a better combustion and a low emission, and these results

provide validity to current tendency that inclines to the highly pressurized injection system.

3.2 Simulation analysis

Figure 7 shows the calculation results of spatial

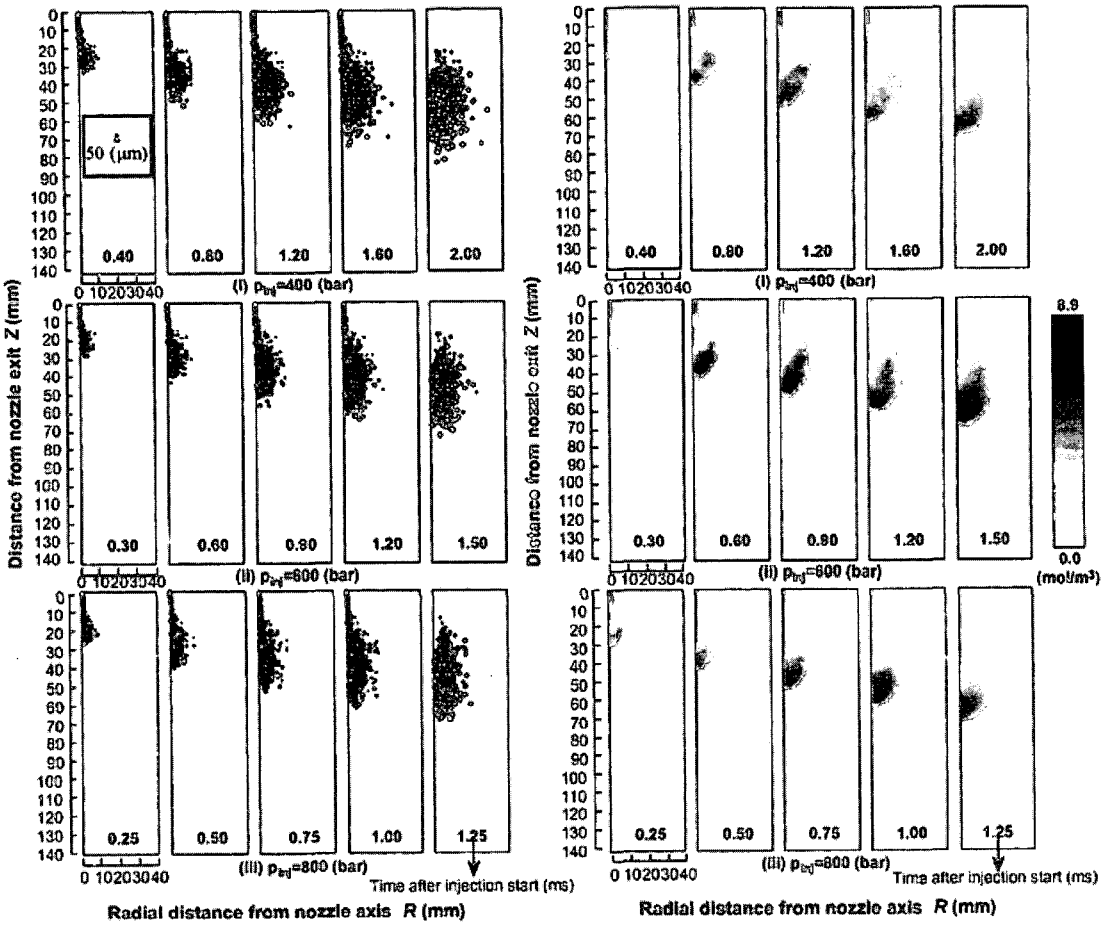

(a) Spatial distribution of droplet parcels (b) Spatial distribution of fuel vapor concentration

Fig. 7 Calculated results of evaporating spray by means of modified KIVA-II code

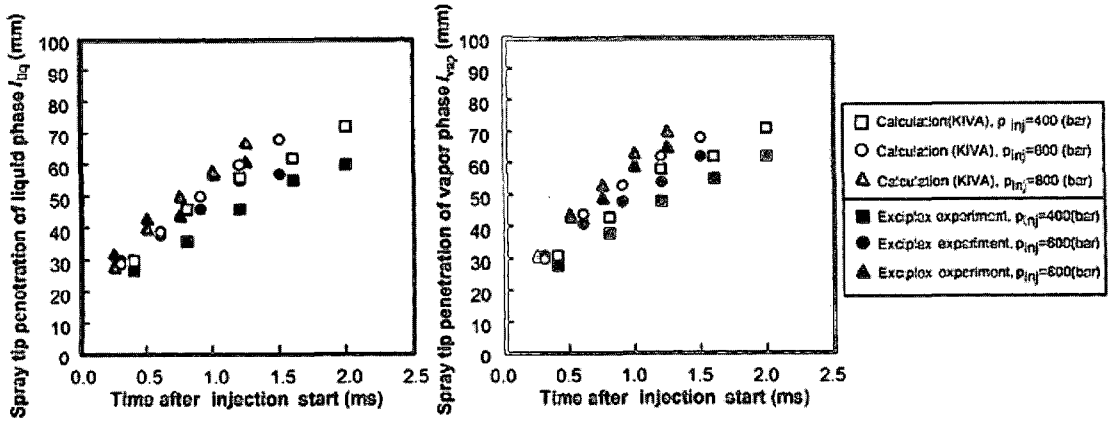

Fig. 8 Comparison of spray tip penetration by means of simulation analysis with experiment results

distribution of droplets and fuel vapor concentration with the modified TAB model. In the figure, the x-axis is the time after injection start with each injection pressure, and y-axis is the distance from nozzle exit. The calculation time was set when the injected fuel mass was almost the same in each injection pressure. The spray tip penetrations of the liquid and vapor phases were almost plotted in the same distance, since momentum is conserved.

In Fig. 8, the spray tip penetrations of liquid and vapor phases are plotted against time after the injection start for the experimental results and the KIVA-II code. The spray tip penetrations of liquid phase (l_{liq}) and vapor phase (l_{vap}) are determined by the overall image distribution region in the figures. Although the results of modified KIVA-II code are slightly different from experimental results, the utility of the KIVA-II code was verified. Hence, the modified TAB model constants of Φ (degree of freedom) =6 and K (energy ratio of particle motion) =0.89, which were applied to evaporating fuel spray, are sufficiently useful for analyzing the macro spray structure.

Figure 9 shows the velocity distribution of droplets by using KIVA-II code in the case of p_{inj}=600 bar. In the figure, the bold arrows express representatively whole flow form of droplets in development process of spray. The velocity vector of droplets near the central spray develops along the central axis of the spray. On the other hand, the velocity distribution of the droplets is turbulent in the periphery of the spray because the droplets lost in the momentum are subject to ambient gas flow. Therefore, it can be also speculated from the results of calculation, the motion of ambient gas is induced by the fuel injection, and the induced motion related to the flow of droplets and vapor fuel dominates the spreading

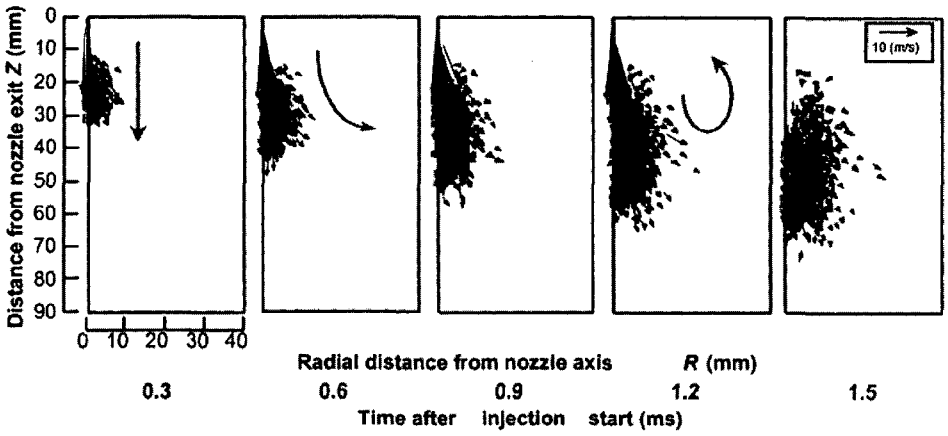

Fig. 9 Temporal change of spatial distribution of droplets velocity (p_{inj}=600 bar, t_{inj}=1.2 ms)

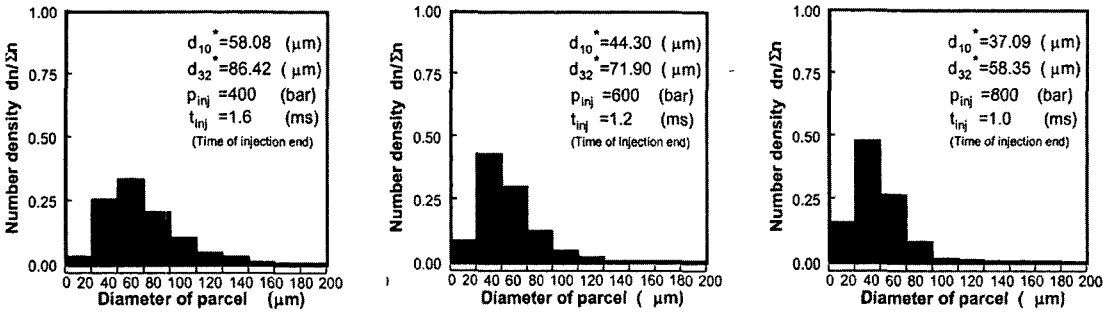

Fig. 10 Change in number density profile with variation of injection pressure obtained by modified TAB model

of the spray.

Figure 10 shows the probability distribution of droplet parcels by using modified KIVA-II code. The probability distributions are the results of injection end in each injection pressure. In this figure, d_{10}^* is arithmetic average ($\sum d_i n_i / \sum n_i$), and d_{32}^* is SMD ($\sum d_i^3 n_i / \sum d_i^2 n_i$), respectively. The parcel diameter of low injection pressure, p_{inj}=400 bar is lager than the one of high injection pressure, p_{inj}=600 and 800 bar. With increasing injection pressure, the range of droplet parcels distribution shifts to small value. In the case of p_{inj}=800 bar, the distribution ratio of $d \leq 40\ \mu m$ is 63% on total diameters. Hence, it can be confirmed that the modified KIVA-II code represents the atomization promotion effect of diesel spray due to the increase of injection pressure, and the utility of the code was verified.

4. Conclusions

An experiment and simulation were performed for the evaporating fuel spray in this study. In the experiment, the exciplex fluorescence method was used, which can simultaneously measure the vapor and liquid phase of the injected fuel. On the other hand, the simulation was performed using the KIVA-II code including modified TAB model.

The following conclusions are drawn from this study.

(1) In the case of the same mass of the injected fuel in the inner spray, the spray tip penetration does not depend on the change of injection pressure.

(2) The liquid length of an evaporating spray converges on a value regardless of the change of injection pressure. In this study, the value is close to 35 mm.

(3) The vapor concentration of injected fuel is leaner due to the increase of atomization in the case of the high injection pressure than in that of the low injection pressure.

(4) The improved TAB model constants of Φ (degree of freedom) =6 and K (energy ratio of particle motion) =0.89, which were applied to evaporating fuel spray, are sufficiently useful for analyzing the macro spray structure.

References

Amsden, A. A., Ramshow, J. D., O'Rourke, P. J. and Dukowiez, J. K., 1985, "KIVA : A Computer Program for Two- and Three-Dimensional Fluid Flows with Chemical Reactions and Fuel Sprays," *Los Alamos National Laboratory Report*, LA-10254-MS.

Amsden, A. A., O'Rourke, P. J. and Butler, T. D., 1989, "KIVA-II : A Computer Program for Chemically Reactive Flows and Sprays," *Los Alamos National Laboratory Report*, LA-11560-MS.

Amsden, A. A., 1993, "KIVA-3 : A KIVA Program with Block-Structured Mesh for Complex Geometries," *Los Alamos National Laboratory Report*, LA-12503-MS.

Amsden, A. A., 1997, "KIVA-3V : A Block-Structured KIVA Program for Engines with Vertical or Canted Valves," *Los Alamos National Laboratory Report*, LA-13313-MS.

Ahmadi-Befrui, B., Uchil, N., Gosman, A. D. and Issa, R., 1996, "Modeling and Simulation of Thin Liquid Films Formed by Spray-Wall Interaction," *SAE Paper*, No. 960627.

Baritaud, T. A., Heinze, T. A. and Le Coz, J. F., 1994, "Spray and Self-Ignition Visualization in a D. I. Diesel Engine," *SAE Paper*, No. 940681.

Dan, T., Takagishi, S., Oishi N., Senda J. and Fujimoto, H., 1996, "The Study of the Spray Structure in the High Injection Pressure," *JSME* 62-597, pp. 2079-2085.

Dan, T., Takagishi, S., Senda, J. and Fujimoto, H., 1997, "Organized Structure and Motion in Diesel Spray," *SAE Paper*, No. 970641.

Espey, C., Dec, J. E., Litzinger, T. A. and Santavicca, D. A., 1994, "Quantitative 2-D Fuel Vapor Concentration Imaging in a Firing D.I. Diesel Engine Using Planar Laser-Induced Rayleigh Scattering," *SAE Paper*, No. 940682.

Espey, C. and Dec, J. E., 1995, "The Effect of TDC Temperature and Density on the Liquid-

Phase Fuel Penetration in a D. I. Diesel Engine," *SAE Paper*, No. 952456.

Espey, C., Dec, J. E., Litzinger, T. A. and Santavicca, D. A., 1997, "Planar Laser Rayleigh Scattering for Quantitative Vapor-Fuel Imaging in a Diesel Jet," *COMBUSTION AND FLAME*, 109 : 65-86, pp. 65~86.

Hiroyasu, H., Kadota, T. and Tasaka, S., 1978, "Study of the Penetration of Diesel Spray," *JSME*, pp. 3208~3219 (in Japanese).

Hiroyasu, H. and Arai, M., 1980, "Fuel Spray Penetration and Spray Angle in Diesel Engines," *JSAE*, No. 21, pp. 5~11 (in Japanese).

Hodges, J. T., Baritaud, T. A. and Heinze, T. A., 1991, "Planar Liquid and Gas Fuel and Droplet Size Visualization in a DI Diesel Engine," *SAE Paper*, No. 910726.

Senda, J., Dan, T., Takagishi, S., Kanda, T. and Fujimoto, H., 1997, "Spray Characteristics of Non-Reacting Diesel Fuel Spray by Experiments and Simulations with KIVA II Code," *Proceedings of ICLASS-'97* (in Seoul), pp. 38~45.

Wakuri, Y., Fujii M., Amitani, T. and Tsuneya R., 1959, "Studies on the Penetration of Fuel Spray of Diesel Engine," *JSME (part2)*, Vol. 52, No. 156, pp. 820~826 (in Japanese).